Research Article

Enhanced Antitumor Immune Response in 2′-5′ Oligoadenylate Synthetase-Like 1- (OASL1-) Deficient Mice upon Cisplatin Chemotherapy and Radiotherapy

Chan Kyu Sim,[1] Jung Hoon Lee,[1] In-Jeoung Baek,[2] Sang-Wook Lee,[3] and Myeong Sup Lee [1]

[1]*Laboratory of Molecular Immunology and Medicine, Department of Biomedical Sciences, University of Ulsan College of Medicine, Asan Medical Center, Seoul 05505, Republic of Korea*
[2]*Department of Convergence Medicine, Asan Institutes for Life Sciences, Asan Medical Center, University of Ulsan College of Medicine, Seoul 05505, Republic of Korea*
[3]*Department of Radiation Oncology, University of Ulsan College of Medicine, Asan Medical Center, Seoul 05505, Republic of Korea*

Correspondence should be addressed to Myeong Sup Lee; myeong@amc.seoul.kr

Type I interferon (IFN-I) plays a critical role in the antitumor immune response. In our previous study, we showed that IFN-I-inducible 2′-5′ oligoadenylate synthetase-like 1 (OASL1) negatively regulated IFN-I production upon tumor challenge similar to that of viral infection. Thus, OASL1-deficient ($Oasl1^{-/-}$) mice were more resistant to implanted tumor growth than wild-type (WT) mice. In this study, we investigated whether targeting or suppressing OASL1 could show synergistic effects on tumor clearance with conventional cancer therapies (such as chemotherapy and radiotherapy) using $Oasl1^{-/-}$ mice and a transplantable lung metastatic tumor cell model. Upon treatment with the anticancer drug cisplatin, we found that $Oasl1^{-/-}$ mice showed enhanced resistance to injected tumors compared to untreated $Oasl1^{-/-}$ mice. Similarly, irradiated $Oasl1^{-/-}$ mice showed better resistance to tumor challenge than untreated $Oasl1^{-/-}$ mice. Additionally, we found that $Oasl1^{-/-}$ mice applied with both types of the cancer therapies contained more cytotoxic effector cells, such as CD8^{+} T cells and NK cells, and produced more cytotoxic effector cytokine IFN-γ as well as IFN-I in their tumor-containing lungs compared to untreated $Oasl1^{-/-}$ mice. Collectively, these results show that targeting OASL1 together with conventional cancer therapies could be an effective strategy to enhance treatment efficacy.

1. Introduction

Conventional cancer therapies, such as chemotherapy and radiotherapy, are still the main treatment options in the clinic [1]. More recently, cancer immunotherapy, which boosts the host's immune response against tumor cells, has emerged as an additional treatment alternative [2]. Popular cancer immunotherapeutic approaches include administration of monoclonal antibodies (Abs) targeting immune checkpoints, adoptive transfer of engineered T cells or tumor-infiltrating lymphocytes (TILs), tumor vaccination, and injection of immune-boosting cytokines or immune adjuvants [3, 4]. Since a single cancer treatment is not effective in many cases, combinational therapy using different approaches is becoming

an important anticancer strategy to completely eradicate cancers in patients [5, 6]. Therefore, diverse combinatorial approaches have been performed in preclinical and clinical investigations [7, 8].

Type I interferon (IFN-I) and its signaling, which are originally known to be essential for antiviral responses, have also been demonstrated to be critical for an effective antitumor immune response [9–11]. Thus, deliveries of exogenous IFN-I and IFN-I-inducing pathogen-associated molecular patterns (PAMPs) were shown to induce enhanced antitumor immune responses [12–16]. Since negative regulators have been shown to affect IFN-I production during viral infections, inhibition of these negative regulators could increase the antitumor immune response [17, 18]. Previously, we have shown

that IFN-I-inducible $2'$-$5'$ oligoadenylate synthetase-like 1 (OASL1), a specific inhibitor of IRF7 (master transcription factor (TF) for IFN-I) translation, negatively regulates IFN-I production upon tumor challenge, similar to those of viral infections [19–22]. As a result, OASL1-deficient ($Oasl1^{-/-}$) mice were more resistant to implanted tumor growth than wild-type (WT) mice [22].

In this study, we evaluated whether standard cancer therapies, such as chemotherapy and radiotherapy, would enhance resistance to implanted tumors in $Oasl1^{-/-}$ mice. We found that $Oasl1^{-/-}$ mice showed more resistance to implanted tumors when treated with cisplatin chemotherapy and radiotherapy than untreated $Oasl1^{-/-}$ mice. This result indicates that OASL1 inhibition can be well integrated with other cancer therapies as a combinatorial treatment.

2. Materials and Methods

2.1. Mice and Cells. $Oasl1^{-/-}$ mice [19] backcrossed to C57BL/6 (The Jackson Laboratory) for ten generations and their littermates were housed in a specific pathogen-free facility. Animal studies were approved by the Institutional Animal Care and Use Committee of Asan Institute for Life Sciences (permit number: 2018-14-046). TC-1, a syngeneic lung epithelial tumor cell line (a gift from T.C. Wu, Johns Hopkins University) established from C57BL/6 lung epithelial cells by expressing HPV oncogenic protein E7 [23], was used. Prior to injection, the cell line was cultured in DMEM supplemented with 10% FBS at 37°C under 5% CO_2.

2.2. In Vivo Tumor Model, Therapy, and Tumor Burden Analysis. To establish an *in vivo* tumor model, TC-1 tumor cells (10^6 cells per mouse) were injected intravenously into the tail of six-to-ten-week-old littermate C57BL/6 wild-type (WT) and $Oasl1^{-/-}$ mice, and mouse health and weight were monitored daily before analysis. A single chemotherapy treatment was applied to mice by intraperitoneal (i.p.) injection of the drug cisplatin (P4394, Sigma-Aldrich) 6 days post-TC-1 tumor injection (d.p.i.). A single radiotherapy treatment was applied to mice at 7 d.p.i. through whole body irradiation using an X-ray irradiator (X-RAD 320, Precision X-Ray Inc.) following anesthesia with Avertin (a mixture of 2,2,2-tribromoethanol (T48402, Sigma-Aldrich) and *tert*-amyl alcohol (PHR1667, Sigma-Aldrich)). To analyze the tumor burden, the left lobe of the lungs was soaked in Bouin's solution (HT10132, Sigma-Aldrich) for more than one day and weighed. Lungs with tumor nodules are heavier than normal lungs.

2.3. FACS Analysis on Immune Cells in Tumor-Containing Lungs. For FACS analysis, the lungs (the right inferior lobe of the lung containing tumor nodules) were collected at the indicated days after TC-1 injection. Subsequently, the lungs were chopped and digested as previously described using 1 mg/mL type II collagenase (C6885, Sigma-Aldrich) and 1 U/mL DNase I (04536282001, Roche) to obtain single cells [22]. To remove red blood cells, the digested single cells were incubated with ACK lysing buffer (1 mL/tissue, A10492-01, Life Technologies) for 5 min at room temperature and then

washed twice with cold DPBS. For staining, the prepared single cells were first Fc blocked ($0.5 \mu L/10^6$ cells) in FACS buffer (DPBS containing 2% FBS) for 20 min at 4°C with CD16/CD32 antibodies (Abs) (2.4G2, BD Pharmingen). Dead cell staining with the Aqua fluorescent reactive dye from the Live/Dead Fixable Dead Cell Stain Kit (L34960, Invitrogen) and surface staining were performed for 30 min at 4°C in the FACS buffer. If necessary, intracellular staining was next performed for 20 min at 4°C using a BD Cytofix/Cytoperm solution kit (554714, BD Pharmingen). The surface staining Abs from BD Pharmingen were CD3e (145-2C11), CD4 (RM4-5), CD8a (53-6.7), CD19 (1D3), NK1.1 (PK136), CD45 (30-F11), CD11c (HL-3), CD45R/B220 (RA3-6B2), and Gr-1 (RB6-8C5); the Abs from eBioscience were CD11b (M1/70) and F4/80 (BM8); and the Ab from Miltenyi Biotec was PDCA-1 (JF05-1C2.4.1). Intracellular staining Abs Foxp3 (FJK-16S) and CD68 (FA-11) were from eBioscience. Stained samples were assessed using FACS-Canto II (BD Biosciences) and further analyzed using FlowJo software (Tree Star).

2.4. FACS Analysis of Apoptotic Cells in Tumor-Containing Lungs. To detect apoptotic cells within nonhematopoietic cells (CD45⁻) which contain mainly tumor cells, the prepared single cells from tumor-containing lungs were Fc blocked and surface stained with the anti-CD45 Ab as described above. Subsequently, the cells were stained with FITC-conjugated Annexin V and 7-AAD using the FITC Annexin V Apoptosis Detection Kit with 7-AAD (640922, BioLegend) following the manufacturer's recommendation. The stained cells were directly analyzed in the FACSCanto II (BD Biosciences).

2.5. RNA Analysis by Quantitative Reverse Transcription PCR (qRT-PCR). Total RNAs ($1.5 \mu g$) purified from tissues using QIAzol RNA isolation reagents (79306, Qiagen) were reverse transcribed for 2 h using oligo dT (20 mer) with SuperScript II Reverse Transcriptase (18064-014, Invitrogen) into cDNAs. Quantitative PCR was performed in the CFX Connect Real-Time PCR Detection System (Br185-5200, Bio-Rad) using gene-specific forward (F) and reverse (R) primers by detecting PCR products with SYBR® Green I gel stain dye (S-7567, Life Technologies) as previously described [22, 24]. The following primers were used: *Gapdh* F: GGCA AATTCAACGGCACAGTCAAG and R: TCGCTCCTGGA AGATGGTGATGG; *IFNg* F: GGCCATCAGCAACAAC ATAAGCGT and R: TGGGTTGTTGACCTCAAACTT GGC; *IFNb1* F: CCACTTGAAGAGCTATTACTG and R: AATGATGAGAAAGTTCCTGAAG; *IFNa5* F: AGGACT CATCTGCTGCATGGAATG and R: CACACAGGCTT TGAGGTCATTGAG; *CXCL9* F: ACATCAGGCTAGGA GTGGTG and R: CACAAGGCTCACGCACAC; *CXCL10* F: CATGAACCCAAGTGCTGCCGTCA and R: TGGATG CAGTTGCAGCGGACCGT; *CXCL11* F: ATCTGGGCCAC AGCTGCTCAAG and R: CTCGATCTCTGCCATTTTG ACGGCTT; and *XCL1* F: GAAGAGAGTAGCTGTGTGA ACTTACAAAC and R: CCCATTTGGCTTCTGGATCAG CACA. The mRNA expression level of each gene was normalized to *Gapdh*.

2.6. *Statistical Analysis.* All data are presented as mean ± standard deviation. All statistical analyses were performed using a two-tailed unpaired Student t test. $p < 0.05$ was considered statistically significant.

3. Results

3.1. *Cisplatin-Treated Oasl1$^{-/-}$ Mice Are More Resistant to TC-1 Lung Metastatic Tumor Challenge.* To explore whether anticancer chemotherapy can further augment the resistance of Oasl1$^{-/-}$ mice to tumor challenge, we employed the TC-1 lung metastasis tumor model used in our previous study, in which TC-1 tumor cells that were introduced into the systemic circulation were deposited in the lung to grow and kill the mice [22, 23]. We chose an anticancer chemotherapeutic agent, cisplatin, one of the most widely used chemotherapeutic agent in clinical practice, for the study [25]. We first determined a therapeutically effective dose of cisplatin in our TC-1 tumor model by a single intraperitoneal (i.p.) injection of cisplatin in wild-type (WT) mice at 6 days post-TC-1 tumor cell injection (d.p.i.) and monitoring survival. Briefly, 25 μg cisplatin-treated WT mice showed a mild improvement in survival (several days), while 100 μg cisplatin-treated WT mice showed a strong survival improvement (about 8 days) (Figure 1(a)). Thus, we chose 100 μg for all of the following experiments. Subsequently, we treated TC-1-injected Oasl1$^{-/-}$ mice and WT mice with cisplatin once at 6 d.p.i. and monitored for survival. As previously shown [22], TC-1-injected Oasl1$^{-/-}$ mice survived about a week longer than WT mice (Figure 1(b)). When cisplatin was treated, Oasl1$^{-/-}$ mice survived much longer (more than 2 weeks) than untreated Oasl1$^{-/-}$ mice (Figure 1(b)).

To determine whether the survival difference was caused by a difference in tumor burden, lung weights, which increase with tumor cell load, were analyzed in mice at 14 d.p.i. (when all 4 groups of mice were still alive) and 21 d.p.i. (when cisplatin-untreated Oasl1$^{-/-}$ mice were still alive). As previously reported, at 14 d.p.i., lung weights of WT mice were heavier than Oasl1$^{-/-}$ mice. As expected, lung weights of cisplatin-treated WT and cisplatin-treated Oasl1$^{-/-}$ mice were lighter than untreated WT and Oasl1$^{-/-}$ mice, respectively (Figure 1(c)). Consistently, at 21 d.p.i., cisplatin-treated Oasl1$^{-/-}$ mice showed much lighter lungs than untreated Oasl1$^{-/-}$ mice (Figure 1(d)). These results together indicate that cisplatin-treated Oasl1$^{-/-}$ mice demonstrate a better antitumor response to metastatic tumor implantation than untreated Oasl1$^{-/-}$ mice.

3.2. *Tumor-Containing Lungs of Cisplatin-Treated Oasl1$^{-/-}$ Mice Contain More Cytotoxic Effector Immune Cells.* To identify the cause of the enhanced resistance in cisplatin-treated Oasl1$^{-/-}$ mice, the major immune cell composition of tumor-containing lungs was analyzed at 21 d.p.i. (when cisplatin-untreated Oasl1$^{-/-}$ mice were still alive) by FACS. The percentage of CD45$^+$ hematopoietic cells in the lungs of cisplatin-treated Oasl1$^{-/-}$ mice at 21 d.p.i. was higher (about 1.5-fold) than those of untreated Oasl1$^{-/-}$ mice (Figures 2(a1) and 2(a2)). Additionally, the proportion of major lymphocytes, such as NK cells, B cells, and CD4$^+$

and CD8$^+$ T cells, within hematopoietic cells was much higher in the lungs of cisplatin-treated Oasl1$^{-/-}$ mice (Figures 2(b1), 2(b2), and 2(b3); see Supplementary Figure 1 for gating strategy). However, the proportion of regulatory T cells (T$_{reg}$; CD3$^+$CD4$^+$Foxp3$^+$) among CD4$^+$ T cells was not significantly changed in the lungs of cisplatin-treated Oasl1$^{-/-}$ mice compared to that of untreated Oasl1$^{-/-}$ mice (Figures 2(c1) and 2(c2)).

Major pulmonary myeloid cell populations were then analyzed at 21 d.p.i. by FACS (see Supplementary Figure 2 for gating strategy) [26]. The proportion of myeloid-derived suppressor cells (MDSCs; broadly defined as CD45$^+$Gr-1$^+$CD11b$^+$ and the most dominant myeloid cells) within CD45$^+$ cells in the lungs of cisplatin-treated Oasl1$^{-/-}$ mice was lower than untreated Oasl1$^{-/-}$ mice (Figures 3(a) and 3(b)). Further, the proportion of alveolar macrophages (AM; CD45$^+$CD68^{hi}CD11c$^+$CD11b$^-$F4/80$^+$Gr-1$^-$) was not significantly different from that of untreated Oasl1$^{-/-}$ mice (Figures 3(a) and 3(b)). However, the proportion of polymorphonuclear cells (PMN; CD45$^+$CD68^{low}CD11b$^+$F4/80$^-$Gr-1^{hi}) and monocytes (Mono; CD45$^+$CD68^{low}CD11b$^+$Gr-1^{low}CD11c$^-$) was higher than that of untreated Oasl1$^{-/-}$ mice (Figures 3(b) and 3(c)). Among the major dendritic cell (DC) populations, the proportions of conventional myeloid DC (mDC; CD45$^+$CD68^{hi}CD11c$^+$F4/80$^-$Gr-1$^-$) and plasmacytoid DC (pDC; CD45$^+$CD11c$^+$B220$^+$PDCA-1$^+$) within CD45$^+$ cells in the lungs of cisplatin-treated Oasl1$^{-/-}$ mice were not significantly different from those of untreated Oasl1$^{-/-}$ mice (Figures 3(b)–3(e1) and 3(e2)). However, the percentage of CD8α^+ DC (CD45$^+$CD11c$^+$B220$^-$CD8α^+CD11b$^-$) within CD45$^+$ cells in the lungs of cisplatin-treated Oasl1$^{-/-}$ mice was much higher than that of untreated Oasl1$^{-/-}$ mice (Figure 3(e1) and 3(e2)).

The observation that CD8$^+$ T and NK cells (cytotoxic effector cells), as well as CD8α^+ DCs (major cells cross-presenting tumor antigen to CD8$^+$ T cells) [27], were present in a much higher proportion, yet the proportion of MDSCs and T$_{reg}$ (immunosuppressive cells) within CD45$^+$ cells were lower or unchanged relative to untreated Oasl1$^{-/-}$ mice, indicates that more effective tumor antigen cross-presentation and cytotoxic CD8$^+$ T cell production occur in the lungs of cisplatin-treated Oasl1$^{-/-}$ mice.

3.3. *Cisplatin-Treated Oasl1$^{-/-}$ Mice Produce More Cytotoxic Effector Cytokine IFN-γ, IFN-I, and Apoptotic Cells in the Tumor-Containing Lungs.* To indirectly investigate the functionality of the CD8$^+$ T and NK cells, the expression of IFN-γ (key cytotoxic effector cytokine) was evaluated in the tumor-containing lungs at 21 d.p.i. by qRT-PCR. The expression level of IFN-γ mRNA was much higher (about 2.5-fold) in the lungs of cisplatin-treated Oasl1$^{-/-}$ mice compared to untreated Oasl1$^{-/-}$ mice (Figure 4(a)), suggesting that cytotoxic CD8$^+$ T and NK cells together are functionally more active in the lungs of cisplatin-treated Oasl1$^{-/-}$ mice. Therefore, enhanced apoptotic cell death is expected in the lungs of cisplatin-treated Oasl1$^{-/-}$ mice. To measure apoptotic cell death directly in the tumor-containing lungs, FACS analysis was performed on single cells derived from the lungs at 21 d.p.i., using 7-AAD/Annexin V to detect apoptotic cells.
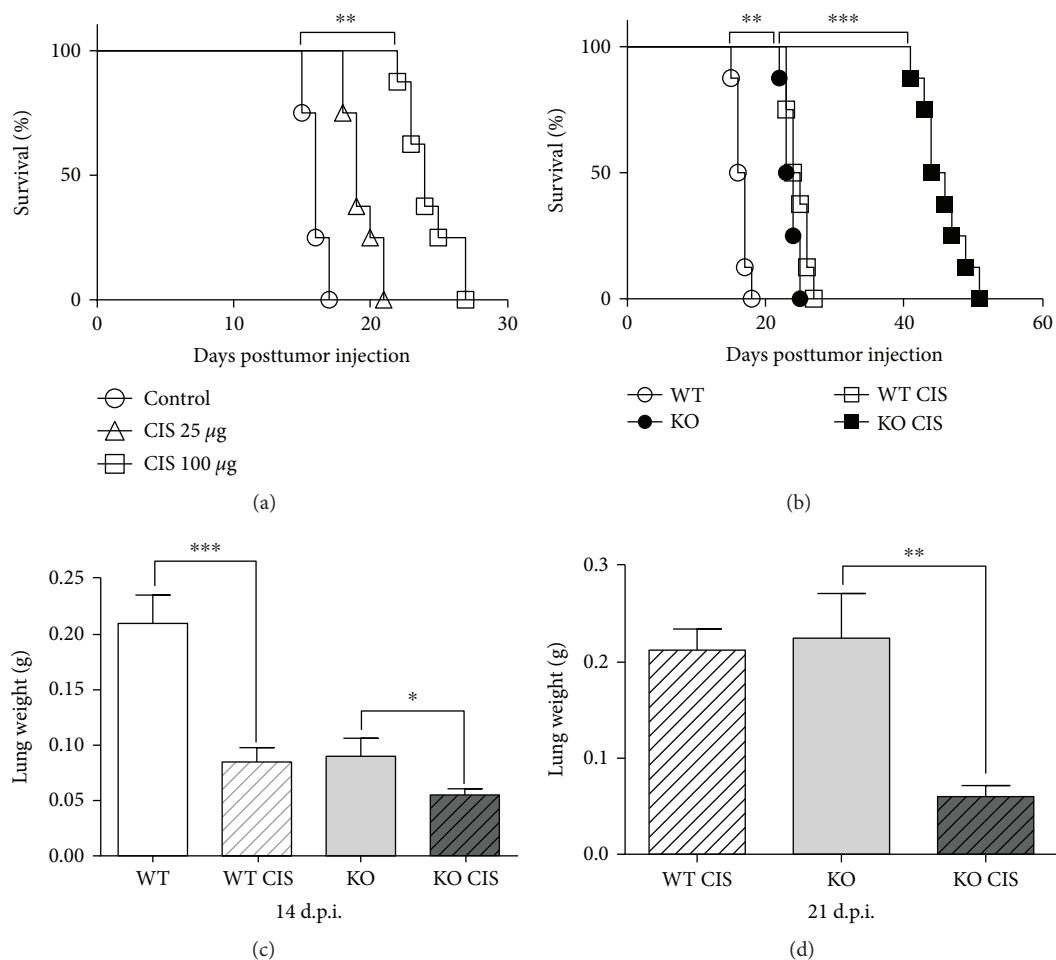
FIGURE 1: Cisplatin-treated $Oasl1^{-/-}$ mice are more resistant to TC-1 lung metastatic tumor challenge. Wild-type (WT) or $Oasl1^{-/-}$ (KO) mice were intravenously injected with TC-1 cells (10^6 cells per mouse), and at 6 days posttumor cell injection (d.p.i.), cisplatin (CIS) was intraperitoneally injected or not. (a) Survival of cisplatin-treated (CIS 25 μg or CIS 100 μg/mice) or untreated (control) TC-1 tumor-bearing WT mice ($n = 8$ per group) was monitored until the indicated day posttumor cell injection. (b) Survival of cisplatin-treated (CIS 100 μg/mice) or untreated TC-1 tumor-bearing WT (WT) and $Oasl1^{-/-}$ mice (KO) ($n = 8$ per group) was observed until the indicated day posttumor cell injection. (c, d) The weights of lungs from cisplatin-treated (CIS 100 μg/mice) or untreated, TC-1 tumor-bearing WT and $Oasl1^{-/-}$ mice ($n = 4$ per group) were measured at 14 (c) and 21 d.p.i. (d). $^*p < 0.05$, $^{**}p < 0.01$, and $^{***}p < 0.001$. Data are representative of at least three independent experiments.

As expected, lungs of cisplatin-treated $Oasl1^{-/-}$ mice contained much more early (Annexin V$^+$/7-AAD$^-$) and late (Annexin V$^+$/7-AAD$^+$) apoptotic cells within nonhematopoietic cells (CD45$^-$ cells, mainly tumor cells) [28, 29] than untreated $Oasl1^{-/-}$ mice (Figures 4(b) and 4(c)). These results indicate that cisplatin-treated $Oasl1^{-/-}$ mice have more tumor-attacking CD8$^+$ T cells and NK cells that can effectively kill growing tumors in the lungs, leading to improved survival of cisplatin-treated $Oasl1^{-/-}$ mice.

We previously showed that tumor-challenged $Oasl1^{-/-}$ mice expressed more IFN-I in the tumor-containing lungs compared to WT mice [22]. Therefore, we investigated whether cisplatin-treated $Oasl1^{-/-}$ mice had increased IFN-I expression in the tumor-containing lungs at 21 d.p.i. The mRNA expression levels of IFN-Is, such as $IFNa5$ and $IFNb1$, in the lungs of cisplatin-treated $Oasl1^{-/-}$ mice were higher (approximately 1.5-fold) than untreated $Oasl1^{-/-}$ mice (Figure 4(d)).

Since IFN-I is known to induce the expression of lymphocyte-recruiting chemokines such as CXCL9, CXCL10, and CXCL11 [30–32], we measured the mRNA expression level of these chemokines in the tumor-containing lungs at 21 d.p.i. The mRNA expression levels were higher (>2-fold) than those in the untreated $Oasl1^{-/-}$ mice (Figure 4(e)). In addition, the mRNA expression level of XCL1 (CD8α$^+$ DC-recruiting chemokine) [33] was higher in the lungs of cisplatin-treated $Oasl1^{-/-}$ mice than in those of untreated $Oasl1^{-/-}$ mice (Figure 4(e)). These results together indicate that the higher number of NK, CD8 T, and CD8α$^+$ DC present in the lungs of cisplatin-treated $Oasl1^{-/-}$ mice is caused, in part, by increased chemokine production in the lungs of cisplatin-treated $Oasl1^{-/-}$ mice compared to untreated $Oasl1^{-/-}$ mice.

3.4. Radiation-Treated Oasl1$^{-/-}$ Mice Are More Resistant to TC-1 Lung Metastatic Tumor Challenge. To explore whether
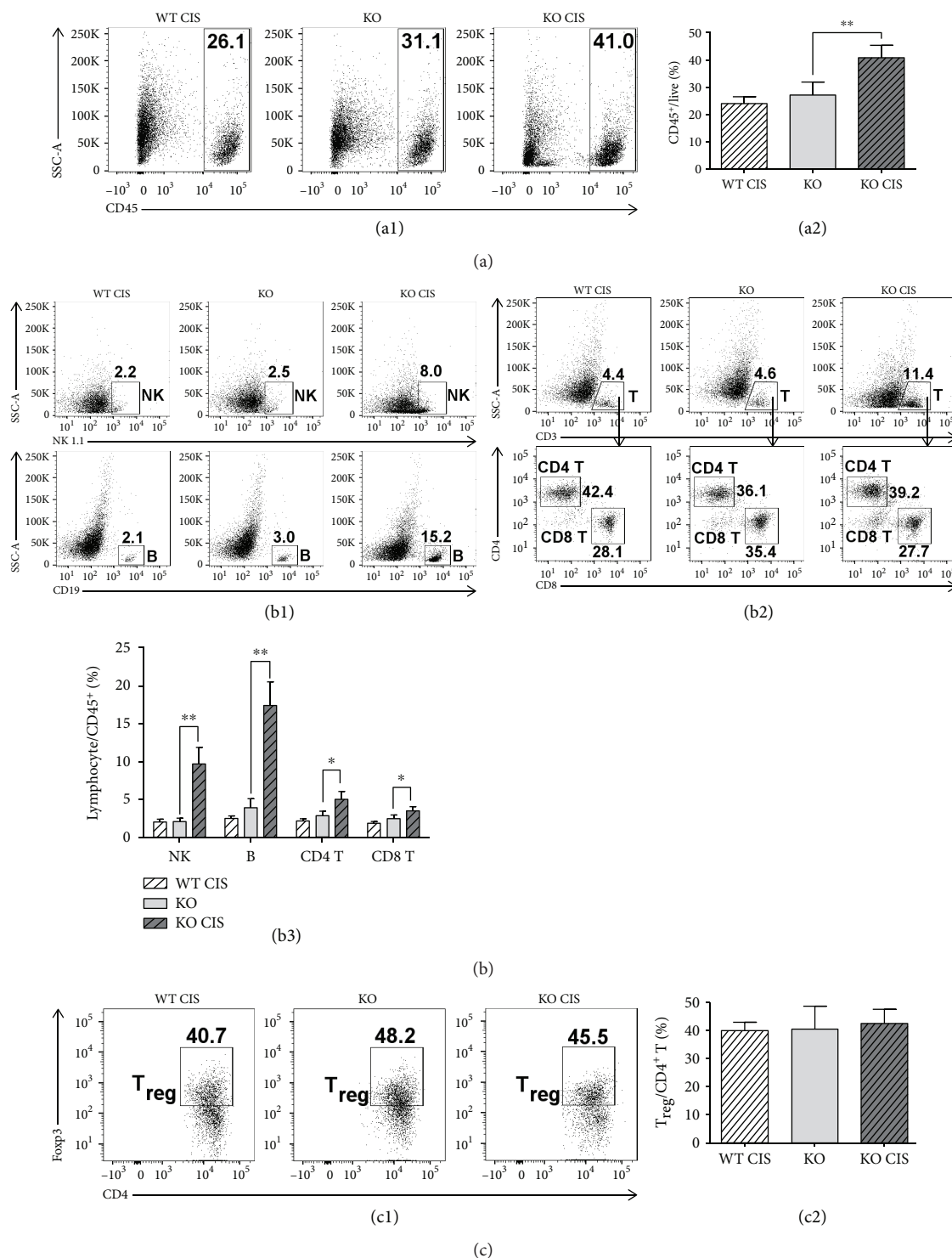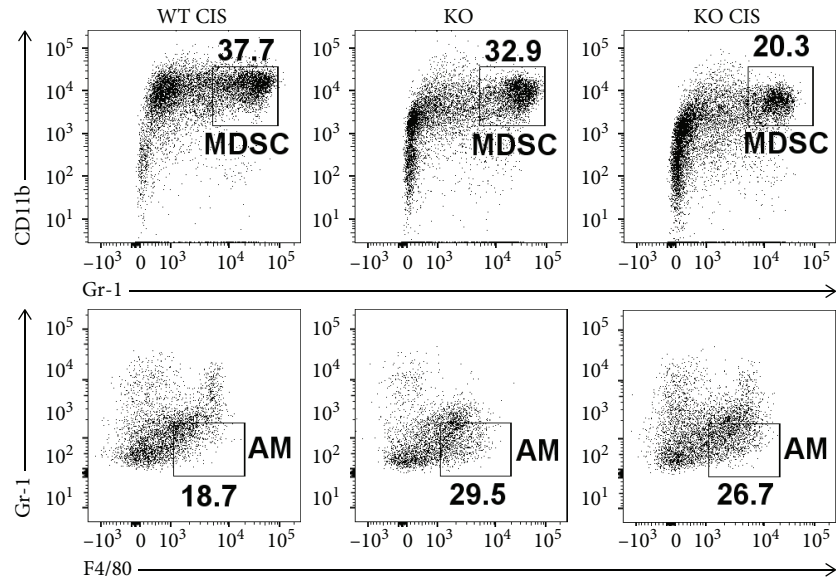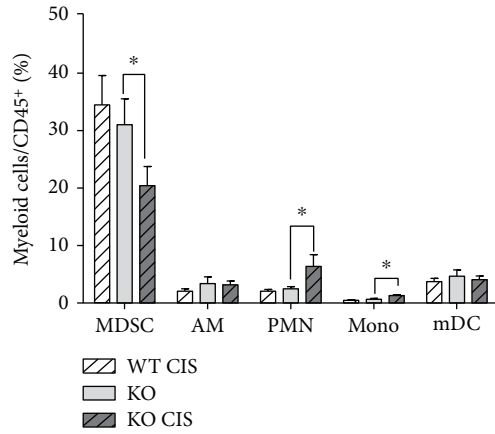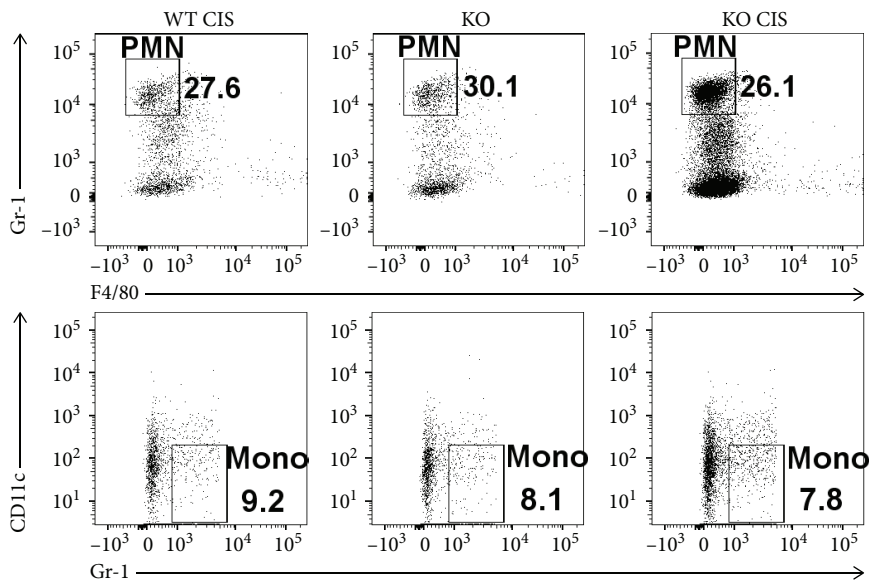
Figure 2: Cisplatin-treated *Oasl1*^{−/−} mice contain more major lymphocyte populations in their tumor-containing lungs than untreated *Oasl1*^{−/−} mice at 21 d.p.i. WT and *Oasl1*^{−/−} (KO) mice were intravenously injected with TC-1 cells (10^6/mouse). At 6 d.p.i., cisplatin-treatment groups of tumor-bearing WT and *Oasl1*^{−/−} mice were intraperitoneally injected with cisplatin (CIS, 100 μg). At 21 d.p.i., the lungs of the mice ($n = 4$ per group) were collected, and the lung-derived single cells were analyzed by FACS. (a) Representative FACS data showing the percentage of CD45^{+} hematopoietic cells among live cells (a1) and summary showing CD45^{+} cell percentage in the tumor-containing lung (a2). (b) Representative FACS data showing the percentages of NK cells (NK1.1^{+}) and B cells (CD19^{+}) and the percentages of T cells (CD3^{+}) among CD45^{+} cells and those of CD4 T cells (CD3^{+}CD4^{+}) and CD8 T cells (CD3^{+}CD8^{+}) within the T cells (b1 and b2); summary showing the percentage of lymphocyte subsets among CD45^{+} cells in the lung (b3). (c) Representative FACS data (c1) and summary (c2) showing the percentage of T_{reg} (CD4^{+}Foxp3^{+}) among CD4^{+} T cells in the lung. $^*p < 0.05$ and $^{**}p < 0.01$. Data are representative of at least three independent experiments.

(a)
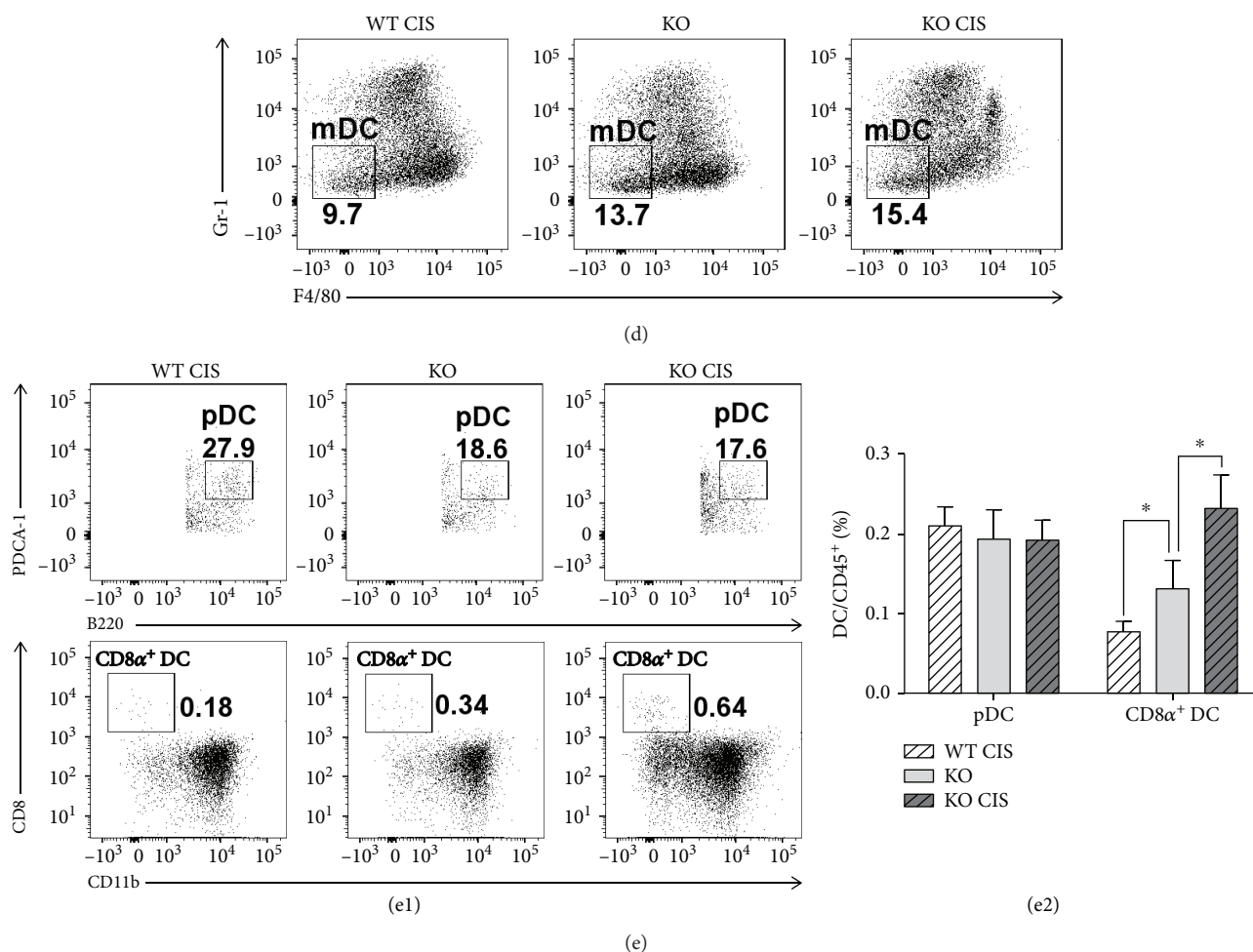

(b)

(c)

Figure 3: Continued.

(d)

(e1)

(e2)

(e)

FIGURE 3: Cisplatin-treated $Oasl1^{-/-}$ mice contain more CD8α^+ DC in their tumor-containing lung than untreated-$Oasl1^{-/-}$ mice. WT and $Oasl1^{-/-}$ (KO) mice ($n = 4$ per group) were intravenously injected with TC-1 cells (10^6/mouse). At 6 d.p.i., cisplatin-treatment groups of tumor-bearing WT and $Oasl1^{-/-}$ mice were intraperitoneally injected with cisplatin (CIS, 100 μg). Subsequently, at 21 d.p.i., lung samples for cisplatin-treated WT mice (WT CIS), untreated $Oasl1^{-/-}$ mice (KO), and cisplatin-treated $Oasl1^{-/-}$ mice (KO CIS) were collected, and the tissue-derived single cells were analyzed by FACS. (a–c) Representative FACS data showing the percentage of myeloid subsets, including (a) MDSC and AM and (c) PMN and monocyte (Mono) among parent populations. (b) The summary data showing the percentage of myeloid subsets and mDC within CD45$^+$ cells. (d) Representative FACS data showing the percentage of mDC within parent population. (e) Representative FACS data showing the percentage of pDC and CD8α^+ DC among their parent populations (e1) and summary data showing the percentage of pDC and CD8α^+ DC within CD45$^+$ cells (e2). $^*p < 0.05$. Data are representative of at least three independent experiments.

radiotherapy, another major conventional cancer therapy, can further augment resistance of $Oasl1^{-/-}$ mice to tumor challenge, we first determined the therapeutically effective radiation dosage in our TC-1 lung metastasis model by irradiating WT mice once at 7 d.p.i. and monitoring survival. Briefly, survival of 4 Gy irradiated WT mice was mildly improved (several days) compared to that of untreated WT mice; however, survival of 6 Gy irradiated WT mice was much higher (about a week) (Figure 5(a)). Thus, we chose 6 Gy for further experiments. When we irradiated TC-1-injected $Oasl1^{-/-}$ mice at this dosage, the irradiated mice survived longer than nonirradiated $Oasl1^{-/-}$ mice (Figure 5(b)). Consistently, tumor burden measured by the lung weights of the mice at 14 d.p.i. was much lighter in the irradiated mice than nonirradiated mice for both $Oasl1^{-/-}$ and WT mice (Figure 5(c)). At 21 d.p.i., when nonirradiated $Oasl1^{-/-}$ mice

were still alive, irradiated $Oasl1^{-/-}$ mice also had much lighter lungs than nonirradiated $Oasl1^{-/-}$ mice (Figure 5(d)). These results indicate that irradiated $Oasl1^{-/-}$ mice demonstrate a better antitumor response to metastatic tumor implantation than untreated $Oasl1^{-/-}$ mice.

3.5. Radiation-Treated $Oasl1^{-/-}$ Mice Contain Higher Cytotoxic Effector Immune Cells in the Tumor-Containing Lungs. To establish the cause for the enhanced resistance of irradiated $Oasl1^{-/-}$ mice, major immune cell composition in tumor-containing lungs was analyzed by FACS. At 21 d.p.i., the percentage of CD45$^+$ hematopoietic cells in the lungs of irradiated $Oasl1^{-/-}$ mice was not significantly different from that of nonirradiated $Oasl1^{-/-}$ mice (Figure 6(a)). However, the proportion of major lymphocytes, such as CD4$^+$ and CD8$^+$ T cells and NK cells, within CD45$^+$
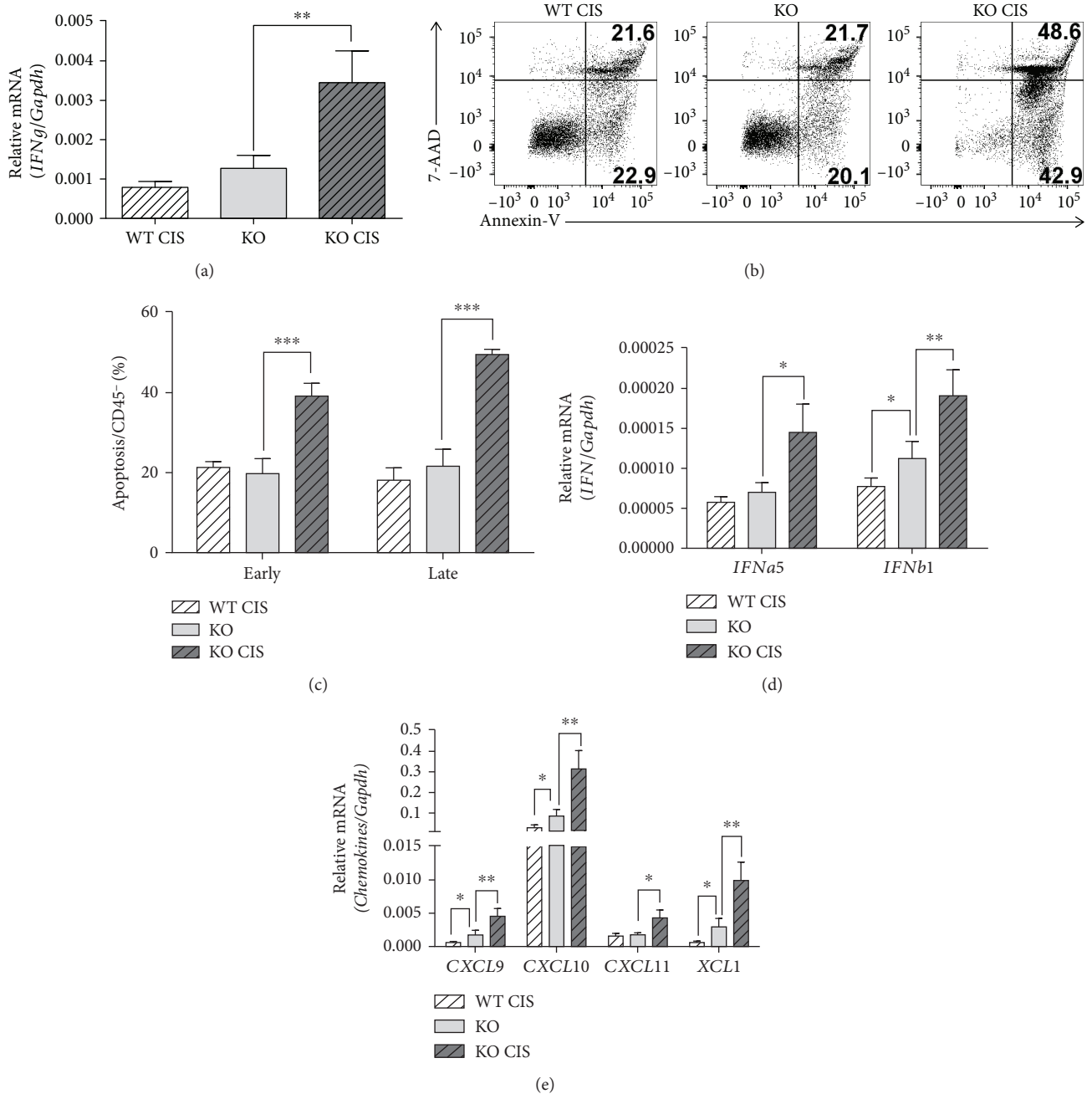
(a)

(b)

(c)

(d)

(e)

FIGURE 4: Cisplatin-treated $Oasl1^{-/-}$ mice have more cytotoxic effector cytokine IFN-γ, IFN-I, and apoptotic cells in the tumor-containing lung. WT and $Oasl1^{-/-}$ mice (KO) were TC-1 injected intravenously (10^6 per mouse), and at 6 d.p.i., cisplatin-treatment groups of tumor-bearing WT and $Oasl1^{-/-}$ mice were intraperitoneally injected with cisplatin (CIS, $100\,\mu$g). At 21 d.p.i., the right middle lobe of the lung for RNA analysis and right inferior lobe of the lung for apoptosis analysis were collected from cisplatin-treated WT (WT CIS), untreated-$Oasl1^{-/-}$ (KO), and cisplatin-treated $Oasl1^{-/-}$ mice (KO CIS). (a) Quantitative RT-PCR analysis of IFN-γ ($IFNg$) mRNA expression at 21 d.p.i. mRNA expression level ($n = 4$ per group) normalized to $Gapdh$ is shown as relative mRNA. (b, c) Representative FACS data showing the percentage of early apoptotic cells (Annexin V$^+$/7-AAD$^-$) and late apoptotic cells (Annexin V$^+$/7-AAD$^+$) among CD45$^-$ cells (b) and summary data ($n = 4$ per group) showing the percentage of two types of apoptotic cells among CD45$^-$ cells (c). (d, e) Quantitative RT-PCR analysis of mRNA expression for $IFNa5$ and $IFNb1$ (d) and for $CXCL9$, $CXCL10$, $CXCL11$, and $XCL1$, at 21 d.p.i. (e). mRNA expression level ($n = 4$ per group) normalized to $Gapdh$ is shown as relative mRNA. $^*p < 0.05$, $^{**}p < 0.01$, and $^{***}p < 0.01$. Data are representative of at least three independent experiments.

hematopoietic cells was much higher (>2-fold) in the lungs of irradiated $Oasl1^{-/-}$ mice. Conversely, the proportion of B cells within CD45$^+$ hematopoietic cells in the lungs of irradiated $Oasl1^{-/-}$ mice were lower (Figure 6(b)), which might be caused by a higher sensitivity of B cells to irradiation [34, 35]. Further, the proportion of T$_{reg}$ within CD4$^+$ T cells was not significantly changed in the lungs of irradiated $Oasl1^{-/-}$ mice (Figure 6(c)). At 21 d.p.i., the proportion of MDSCs was
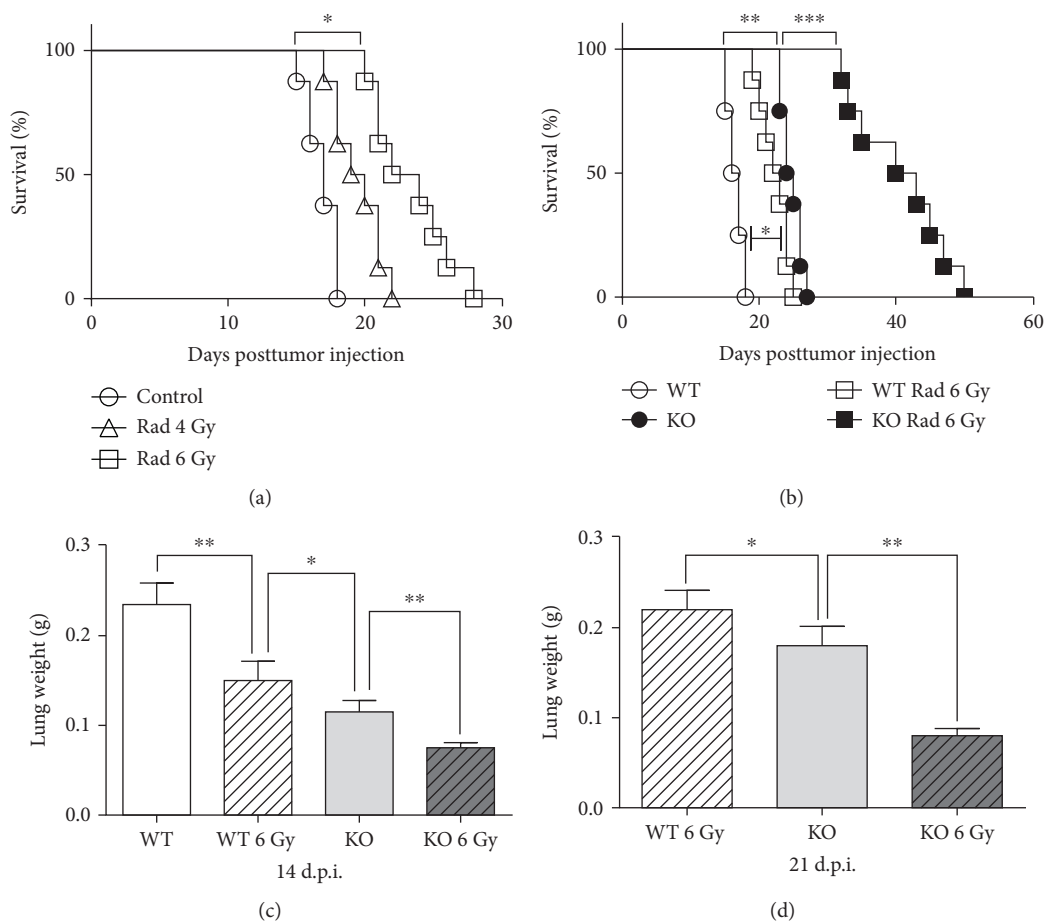
(a)

(b)

(c)

(d)

FIGURE 5: Irradiated $Oasl1^{-/-}$ mice are more resistant to TC-1 tumor challenge than nonirradiated $Oasl1^{-/-}$ mice. WT and $Oasl1^{-/-}$ mice were TC-1 injected intravenously (10^6 per mouse), and irradiation was performed on day 7 post-TC-1 injection to anesthetized mice. (a) Survival of nonirradiated (control) and irradiated (Rad 4 Gy or Rad 6 Gy) tumor-bearing WT mice was observed until the indicated days to determine the proper irradiation dosage. (b) Survival of nonirradiated (WT and KO) and 6 Gy irradiated tumor-bearing WT (WT Rad 6 Gy) and $Oasl1^{-/-}$ mice (KO Rad 6 Gy) was monitored until the indicated days. (c, d) The weight of the left lobe of the lung from untreated and 6 Gy irradiated tumor-bearing WT (WT 6 Gy) and $Oasl1^{-/-}$ mice (KO 6 Gy) was measured at 14 (c) and 21 d.p.i. (d). $^*p < 0.05$, $^{**}p < 0.01$, and $^{***}p < 0.001$. Data are representative of at least three independent experiments.

lower than that of untreated $Oasl1^{-/-}$ mice, while the proportion of AM within CD45$^+$ cells in the lungs of irradiated $Oasl1^{-/-}$ mice were not significantly different from that of untreated $Oasl1^{-/-}$ mice (Figure 6(d)). However, the proportions of PMN and monocytes within CD45$^+$ cells in the lungs of irradiated $Oasl1^{-/-}$ mice were slightly higher than those of untreated $Oasl1^{-/-}$ mice (Figure 6(d)). Among major dendritic cell populations, the proportion of mDC within CD45$^+$ cells in the lungs of cisplatin-treated $Oasl1^{-/-}$ mice was not significantly different from that of untreated $Oasl1^{-/-}$ mice (Figure 6(d)). However, the proportions of pDC and CD8α^+ DC within CD45$^+$ cells in the lungs of irradiated $Oasl1^{-/-}$ mice were higher than those of untreated $Oasl1^{-/-}$ mice (Figure 6(e)). Similar to cisplatin-treated $Oasl1^{-/-}$ mice, CD8$^+$ T and NK cells (cytotoxic effector cells), as well as CD8α^+ DCs (major cells cross-presenting tumor antigen to CD8$^+$ T cells), which were present in a much higher proportion within CD45$^+$ cells in the lungs of irradiated $Oasl1^{-/-}$ mice, and MDSCs (present in a lower number in the lungs of irradiated $Oasl1^{-/-}$ mice) might contribute to the more

effective antitumor immune response in the irradiated $Oasl1^{-/-}$ mice.

3.6. Radiation-Treated $Oasl1^{-/-}$ Mice Produce More IFN-γ, IFN-I, and Apoptotic Cells in the Tumor-Containing Lungs.

To indirectly investigate the functionality of cytotoxic immune cells, IFN-γ expression was evaluated in the tumor-containing lungs at 21 d.p.i. by qRT-PCR. The expression level of IFN-γ mRNA was much higher in the lungs of irradiated $Oasl1^{-/-}$ mice compared to untreated $Oasl1^{-/-}$ mice (Figure 7(a)), indicating that cytotoxic cells were functionally more active in the lungs of irradiated $Oasl1^{-/-}$ mice. Consistently, the lungs of irradiated $Oasl1^{-/-}$ mice contained much more apoptotic cells within nonhematopoietic cells (CD45$^-$ cells) than those of untreated $Oasl1^{-/-}$ mice (Figure 7(b)). These results indicate that irradiated $Oasl1^{-/-}$ mice have more tumor-attacking cytotoxic cells, such as CD8$^+$ T cells and NK cells, that can kill growing tumors in the lungs, leading to the improved survival of irradiated $Oasl1^{-/-}$ mice.
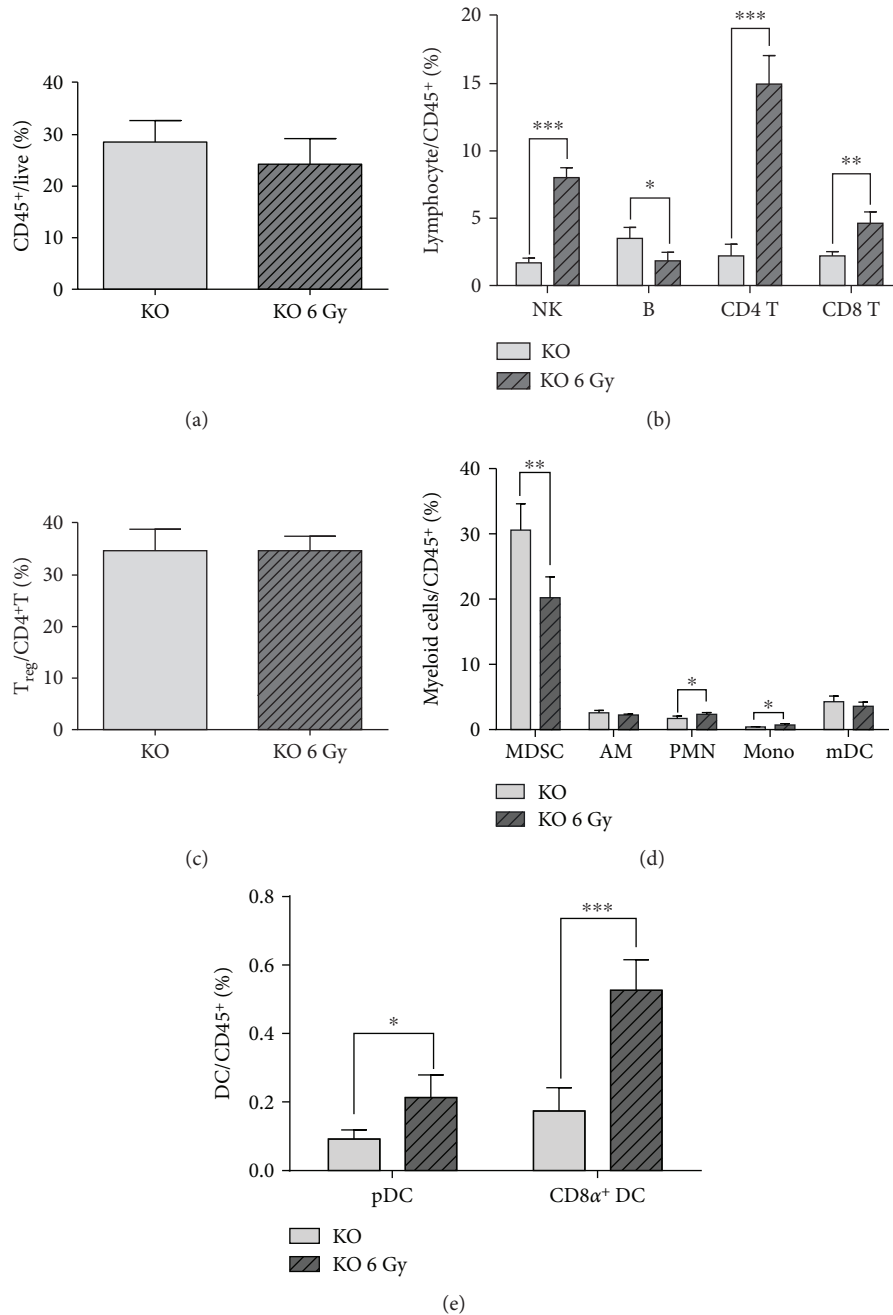
(a)

(b)

(c)

(d)

(e)

Figure 6: Irradiated $Oasl1^{-/-}$ mice contain higher cytotoxic effector immune cells in the tumor-containing lungs. WT and $Oasl1^{-/-}$ (KO) mice ($n = 4$ per group) were intravenously injected with TC-1 tumor cells (10^6/mouse). At 7 d.p.i., the radiation-treatment groups of tumor-bearing WT and $Oasl1^{-/-}$ mice received 6 Gy whole body irradiation. At 21 d.p.i., the right inferior lobe of the lung was collected, and the lung-derived single cells were analyzed by FACS. (a) Summary of FACS data showing the percentage of CD45$^+$ cells among live cells in the tumor-containing lung. (b) Summary of FACS data showing the percentage of NK cells (NK1.1$^+$), B cells (CD19$^+$), CD4 T cells (CD3$^+$CD4$^+$), and CD8 T cells (CD3$^+$CD8$^+$) among CD45$^+$ cells. (c) Summary of FACS data showing the percentage of T$_{reg}$ (CD4$^+$Foxp3$^+$) among CD4$^+$ T cells in the lung. (d) Summary of FACS data showing the percentage of MDSC, AM, PMN, Mono, and mDC among CD45$^+$ cells. (e) Summary of FACS data showing the percentage of pDC and CD8α^+ DC among CD45$^+$ cells. $^*p < 0.05$, $^{**}p < 0.01$, and $^{***}p < 0.001$. Data are representative of at least three independent experiments.

We next investigated whether the enhanced antitumor immune response observed in the lungs of irradiated $Oasl1^{-/-}$ mice may be caused by increased IFN-I expression, similar to cisplatin-treated $Oasl1^{-/-}$ mice. Indeed, the mRNA expression levels of IFN-Is, such as $IFNa5$ and $IFNb1$, in the lungs of irradiated $Oasl1^{-/-}$ mice at 21 d.p.i., were higher (approximately 1.4-fold) than those of untreated $Oasl1^{-/-}$ mice (Figure 7(c)).
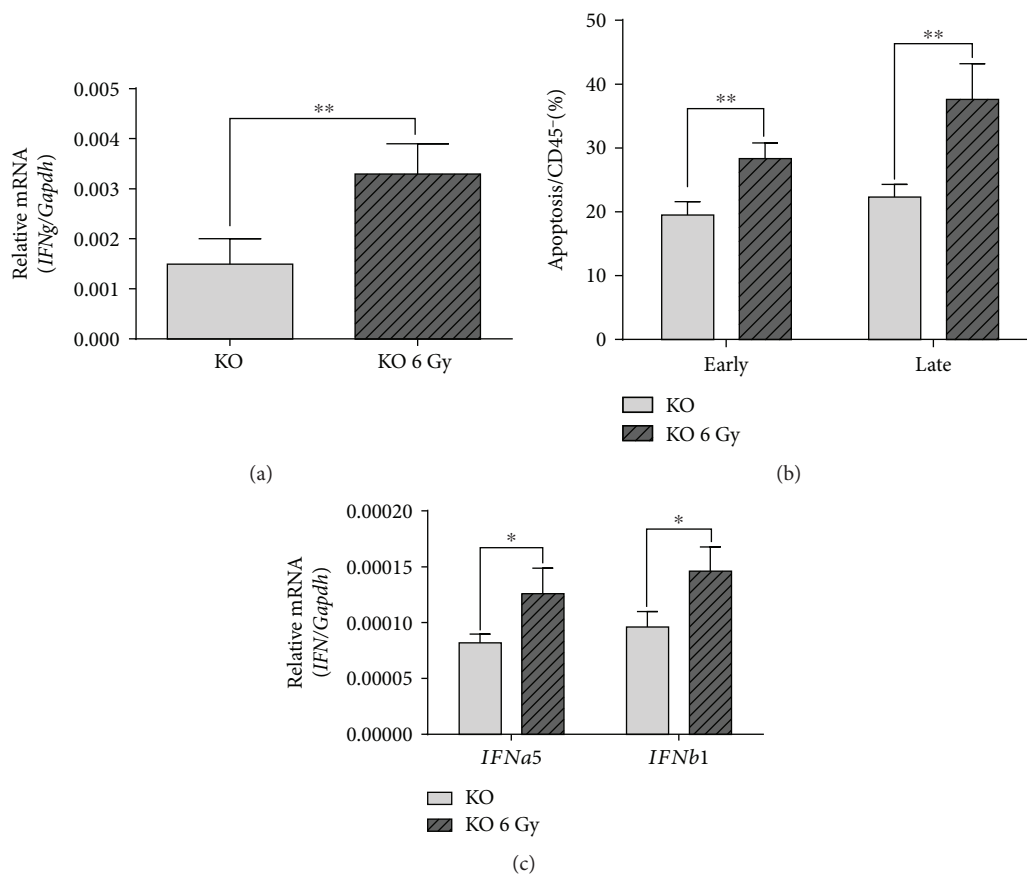
(a)

(b)

(c)

FIGURE 7: Irradiated $Oasl1^{-/-}$ mice produce more IFN-γ, IFN-I, and apoptotic cells in the tumor-containing lung. WT and $Oasl1^{-/-}$ (KO) mice ($n = 4$ per group) were intravenously injected with TC-1 tumor cells (10^6/mouse). At 7 d.p.i., the radiation-treatment groups of tumor-bearing WT and $Oasl1^{-/-}$ mice received 6 Gy whole body irradiation. At 21 d.p.i., the right middle lobe of the lung was collected for RNA analysis and the right inferior lobe of the lung was collected for FACS analysis. (a–c) Quantitative RT-PCR analysis of mRNA expression for $IFNg$ (a) and $IFNa5$ and $IFNb1$ (c); mRNA expression level ($n = 4$ per group) normalized to $Gapdh$ is shown as relative mRNA. (b) Summary data ($n = 4$ per group) showing the percentage for two types of apoptotic cells among CD45$^-$ cells; early apoptotic cells (Annexin V$^+$/7-AAD$^-$) and late apoptotic cells (Annexin V$^+$/7-AAD$^+$). $^*p < 0.05$, $^{**}p < 0.01$, and $^{***}p < 0.001$. Data are representative of at least three independent experiments.

4. Discussion

In this study, we evaluated whether the resistance of $Oasl1^{-/-}$ mice to implanted tumors can be further improved with conventional cancer therapies such as chemotherapy and radiotherapy. We found that $Oasl1^{-/-}$ mice showed more resistance to implanted tumors when treated with a representative chemotherapeutic agent cisplatin, as well as irradiation, than untreated $Oasl1^{-/-}$ mice. Additionally, we found that antitumor cytotoxic effector cells, such as CD8$^+$ T cells and NK cells, as well as CD8α^+ DCs (major antigen cross-presenting cells), were more abundant in the tumor-containing lungs of cisplatin-treated and irradiated $Oasl1^{-/-}$ mice than untreated $Oasl1^{-/-}$ mice. However, the proportions of immunosuppressive MDSCs within the hematopoietic cells and T$_{reg}$ within CD4$^+$ T cells in the therapy-applied $Oasl1^{-/-}$ lungs were lower or similar, respectively, to those of untreated $Oasl1^{-/-}$ mice. Consistently, the mRNA expression of cytotoxic effector cytokine IFN-γ, produced by functionally active CD8$^+$ T and NK cells, was higher in the therapy-applied $Oasl1^{-/-}$ lungs, and more

apoptotic nonhematopoietic cells (that are thought to be mainly tumor cells) [28, 29] were observed in the therapy-applied lungs of $Oasl1^{-/-}$ mice compared to untreated $Oasl1^{-/-}$ mice.

In our previous study, we demonstrated that $Oasl1^{-/-}$ mice produced higher levels of IFN-I and were more resistant to the TC-1 tumor challenge than WT mice [22]. In our current study, we showed that cisplatin-treated or irradiated $Oasl1^{-/-}$ mice expressed higher levels of IFN-I in the tumor-containing lungs than untreated $Oasl1^{-/-}$ mice, indicating that there is synergy between OASL1 deficiency and cisplatin treatment or irradiation for IFN-1 expression. Cisplatin and irradiation can directly kill growing tumor cells [36, 37], thus more tumor antigen and danger-associated molecular patterns (DAMPs), including tumor cell DNAs, ATP, and HMGB1, would be released from dying tumor cells in the therapy-applied $Oasl1^{-/-}$ lungs [36–38]. Tumor cell-derived DNAs can be detected by one of the major DNA sensors, cyclic GMP-AMP synthase (cGAS) (a cytosolic DNA sensor), which activates STING and then the TBK1 (the major kinase for IRF7 and IRF3 activation) pathway, thus

inducing IFN-1 expression [39, 40]. According to our previous study using the same tumor model, pDC, which can predominantly produce large amounts of IFN-I because of its high basal expression of IRF7 [41, 42], was the main producer of IFN-I in tumors [22]. Thus, the cGAS-STING-TBK1-IRF7 pathway in pDC might also be responsible for IFN-I expression in the cisplatin-treated and irradiated tumor-containing lungs of $Oasl1^{-/-}$ mice, although we cannot rule out the possibility of the contribution of the TLR9-Myd88-IRF7 pathway, which can detect extracellular DNA in pDC [43, 44]. Regardless of the mechanism to detect the tumor cell DNA, the higher number of pDCs present in cisplatin-treated $Oasl1^{-/-}$ lungs (a greater number of CD45$^+$ cells present in the lungs and a similar percentage of pDC within CD45$^+$ cells lead to a higher number of pDCs in the lungs) and irradiation-treated $Oasl1^{-/-}$ lungs (similar number of CD45$^+$ cells present in lungs and higher percentage of pDC within CD45$^+$ cells lead to higher number of pDCs in the lungs) compared to untreated $Oasl1^{-/-}$ lungs, together with the higher availability of tumor cell-derived DNA for the pDC activation, would considerably contribute to the observed enhanced IFN-I expression in the therapy-applied $Oasl1^{-/-}$ lungs.

IFN-I is a potent immunostimulator that enhances host antitumor immune responses [10, 45]. IFN-I can promote the tumor antigen cross-presentation to naïve CD8$^+$ T cells by stimulating DC (including CD8α^+ DCs) maturation and migration to lymph nodes and thus clonal expansion and differentiation into cytotoxic effector CD8$^+$ T cells indirectly. IFN-I can also directly enhance clonal expansion of antigen-experienced CD8$^+$ T cells and enhance CD8$^+$ T cell cytotoxicity [46, 47]. Additionally, IFN-I can directly promote CD4$^+$ T cell expansion and Th1 (type 1 T helper) cell differentiation [45, 48] and indirectly promote the expansion and survival of NK cells through the induction of IL-15 expression [49, 50]. Furthermore, IFN-I can promote B cell survival, differentiation, and function and inhibit the immunosuppressive function of T$_{reg}$ [10, 51]. Collectively, these facts indicate that the higher amount of IFN-I present in the therapy-applied $Oasl1^{-/-}$ lungs would stimulate both innate and adaptive immune cells and provide a higher number and better functioning of cytotoxic effector cells to the therapy-applied $Oasl1^{-/-}$ lungs, leading to improved tumor resistance and better survival of the treated $Oasl1^{-/-}$ mice.

We used cisplatin as a main anticancer chemotherapeutic agent in this study. Cisplatin, a widely used chemotherapeutic agent in clinical practice, can cross-link DNA and directly induce apoptotic tumor cell death [25]. In addition to the direct cytotoxic activity, cisplatin can modulate the immune system to enhance the antitumor response [25, 36]. It can induce MHC I upregulation on the tumor and antigen-presenting cells. Further, it promotes proliferation and recruitment of immune effector cells, such as CD8$^+$ T and NK cells. Finally, it enhances the lytic activity of cytotoxic effector cells and reduces the number of MDSC cells. Thus, the synergistic antitumor effect observed between OASL1 deficiency and cisplatin is thought to be caused by the combination of IFN-I's immune-boosting effects as well as cisplatin's direct cytotoxicity and indirect immune-boosting functions. Other chemotherapeutic agents showing immune-boosting roles in addition to the tumor cell cytotoxicity are worth exploring for potential synergy with OASL1 deficiency in the future [52, 53].

We also tested whether another major conventional cancer therapy, radiotherapy, can add an anticancer therapeutic benefit with OASL1 deficiency. Similar to cisplatin treatment, radiation increased the anticancer therapeutic benefits of OASL1 deficiency. This result indicates that OASL1 inhibition could be well integrated with conventional anticancer therapies as a combinatorial treatment. Although we did not explore the possibility of the potential synergy between OASL1 deficiency and targeted therapy or other immunotherapy in this study, OASL1 deficiency may show a good synergy with at least some of such therapies because IFN-I delivery has been shown to add a benefit to the targeted therapies using EGFR-targeting Abs (erlotinib and nimotuzumab) [54] and BRAF inhibitor [55] and immunotherapies using anti-PD-1 and anti-CTLA-4 Abs [56].

OASL1 is a translation inhibitor of IRF7, the IFN-inducible IFN-I master TF. Thus, it negatively regulates robust IFN-I production upon virus and tumor challenge [19–22]. Since there are other negative regulators acting on the process of IFN-I production and/or IFN-I receptor signaling pathway [17, 18], inhibitors of these other negative regulators might be useful together with conventional anticancer therapies to achieve a synergistic antitumor effect. Thus, developing specific inhibitors for such negative regulators, including OASL1, is worthy of investigation in the future.

5. Conclusions

In this study, we investigated whether suppression of OASL1 showed a synergistic effect on tumor clearance with the conventional cancer therapies, chemotherapy and radiotherapy, using $Oasl1^{-/-}$ mice and a lung metastatic tumor cell model. We found that $Oasl1^{-/-}$ mice treated with the anticancer drug cisplatin and irradiated $Oasl1^{-/-}$ mice showed enhanced resistance to injected tumors compared to untreated $Oasl1^{-/-}$ mice. We also found that the therapy-applied $Oasl1^{-/-}$ mice contained more cytotoxic effector cells, such as CD8$^+$ T cells and NK cells, and produced more cytotoxic effector cytokine IFN-γ as well as IFN-I in their tumor-containing lungs compared to untreated $Oasl1^{-/-}$ mice. Collectively, these results show that OASL1-targeted therapy together with conventional cancer therapies could enhance tumor treatment efficacy.

Data Availability

The data used to support the findings of this study are available from the corresponding author upon request.

Conflicts of Interest

The authors declare that there is no conflict of interest regarding the publication of this article.

Acknowledgments

Supplementary Materials

Supplementary Figure 1: gating strategy used to identify major lymphocyte populations of NK, B, CD3$^+$ T, CD4$^+$ T, CD8$^+$ T, and T$_{reg}$ cells. Supplementary Figure 2: gating strategy used to identify major pulmonary myeloid populations of PMN, monocytes (Mono), AM, mDC, and MDSC from tumor-containing mouse lung tissues. *(Supplementary Materials)*

References

[1] A. Urruticoechea, R. Alemany, J. Balart, A. Villanueva, F. Vinals, and G. Capella, "Recent advances in cancer therapy: an overview.," *Current pharmaceutical design*, vol. 16, no. 1, pp. 3–10, 2010.

[2] D. N. Khalil, E. L. Smith, R. J. Brentjens, and J. D. Wolchok, "The future of cancer treatment: immunomodulation, CARs and combination immunotherapy," *Nature Reviews. Clinical Oncology*, vol. 13, no. 6, p. 394, 2016.

[3] F. Ito and A. E. Chang, "Cancer immunotherapy: current status and future directions," *Surgical Oncology Clinics of North America*, vol. 22, no. 4, pp. 765–783, 2013.

[4] S. Farkona, E. P. Diamandis, and I. M. Blasutig, "Cancer immunotherapy: the beginning of the end of cancer?," *BMC Medicine*, vol. 14, no. 1, p. 73, 2016.

[5] M. Vanneman and G. Dranoff, "Combining immunotherapy and targeted therapies in cancer treatment," *Nature Reviews Cancer*, vol. 12, no. 4, pp. 237–251, 2012.

[6] S. B. Coffelt and K. E. de Visser, "Immune-mediated mechanisms influencing the efficacy of anticancer therapies," *Trends in Immunology*, vol. 36, no. 4, pp. 198–216, 2015.

[7] A. E. Vilgelm, D. B. Johnson, and A. Richmond, "Combinatorial approach to cancer immunotherapy: strength in numbers," *Journal of Leukocyte Biology*, vol. 100, no. 2, pp. 275–290, 2016.

[8] P. A. Ott, F. S. Hodi, H. L. Kaufman, J. M. Wigginton, and J. D. Wolchok, "Combination immunotherapy: a road map," *Journal for ImmunoTherapy of Cancer*, vol. 5, no. 1, p. 16, 2017.

[9] M. S. Lee and Y. J. Kim, "Signaling pathways downstream of pattern-recognition receptors and their cross talk," *Annual Review of Biochemistry*, vol. 76, no. 1, pp. 447–480, 2007.

[10] L. Zitvogel, L. Galluzzi, O. Kepp, M. J. Smyth, and G. Kroemer, "Type I interferons in anticancer immunity," *Nature Reviews Immunology*, vol. 15, no. 7, pp. 405–414, 2015.

[11] K. J. Zhang, X. F. Yin, Y. Q. Yang et al., "A potent *in vivo* antitumor efficacy of novel recombinant type I interferon," *Clinical Cancer Research*, vol. 23, no. 8, pp. 2038–2049, 2017.

[12] F. Aranda, E. Vacchelli, F. Obrist et al., "Trial watch: Toll-like receptor agonists in oncological indications," *OncoImmunology*, vol. 3, no. 6, article e29179, 2014.

[13] L. Deng, H. Liang, M. Xu et al., "STING-dependent cytosolic DNA sensing promotes radiation-induced type I interferon-dependent antitumor immunity in immunogenic tumors," *Immunity*, vol. 41, no. 5, pp. 843–852, 2014.

[14] H. Hashimoto, R. Ueda, K. Narumi, Y. Heike, T. Yoshida, and K. Aoki, "Type I IFN gene delivery suppresses regulatory T cells within tumors," *Cancer Gene Therapy*, vol. 21, no. 12, pp. 532–541, 2014.

[15] C. Xu, L. Lin, G. Cao et al., "Interferon-α-secreting mesenchymal stem cells exert potent antitumor effect in vivo," *Oncogene*, vol. 33, no. 42, pp. 5047–5052, 2014.

[16] A. Cauwels, S. van Lint, F. Paul et al., "Delivering type I interferon to dendritic cells empowers tumor eradication and immune combination treatments," *Cancer Research*, vol. 78, no. 2, pp. 463–474, 2018.

[17] R. A. Porritt and P. J. Hertzog, "Dynamic control of type I IFN signalling by an integrated network of negative regulators," *Trends in Immunology*, vol. 36, no. 3, pp. 150–160, 2015.

[18] K. I. Arimoto, S. Miyauchi, S. A. Stoner, J. B. Fan, and D. E. Zhang, "Negative regulation of type I IFN signaling," *Journal of Leukocyte Biology*, vol. 103, no. 6, pp. 1099–1116, 2018.

[19] M. S. Lee, B. Kim, G. T. Oh, and Y. J. Kim, "OASL1 inhibits translation of the type I interferon-regulating transcription factor IRF7," *Nature Immunology*, vol. 14, no. 4, pp. 346–355, 2013.

[20] M. S. Lee, C. H. Park, Y. H. Jeong, Y. J. Kim, and S. J. Ha, "Negative regulation of type I IFN expression by OASL1 permits chronic viral infection and CD8$^+$ T-cell exhaustion," *PLoS Pathogens*, vol. 9, no. 7, article e1003478, 2013.

[21] J. E. Oh, M. S. Lee, Y. J. Kim, and H. K. Lee, "OASL1 deficiency promotes antiviral protection against genital herpes simplex virus type 2 infection by enhancing type I interferon production," *Scientific Reports*, vol. 6, no. 1, article 19089, 2016.

[22] C. K. Sim, Y. S. Cho, B. S. Kim, I. J. Baek, Y. J. Kim, and M. S. Lee, "2′-5′ Oligoadenylate synthetase-like 1 (OASL1) deficiency in mice promotes an effective anti-tumor immune response by enhancing the production of type I interferons," *Cancer Immunology, Immunotherapy*, vol. 65, no. 6, pp. 663–675, 2016.

[23] H. Ji, E. Y. Chang, K. Y. Lin, R. J. Kurman, D. M. Pardoll, and T. C. Wu, "Antigen-specific immunotherapy for murine lung metastatic tumors expressing human papillomavirus type 16 E7 oncoprotein," *International Journal of Cancer*, vol. 78, no. 1, pp. 41–45, 1998.

[24] Y. S. Cho, B. S. Kim, C. K. Sim, I. Kim, and M. S. Lee, "Establishment of IL-7 expression reporter human cell lines, and their feasibility for high-throughput screening of IL-7-upregulating chemicals," *PLoS One*, vol. 11, no. 9, article e0161899, 2016.

[25] A. R. de Biasi, J. Villena-Vargas, and P. S. Adusumilli, "Cisplatin-induced antitumor immunomodulation: a review of preclinical and clinical evidence," *Clinical Cancer Research*, vol. 20, no. 21, pp. 5384–5391, 2014.

[26] R. Zaynagetdinov, T. P. Sherrill, P. L. Kendall et al., "Identification of myeloid cell subsets in murine lungs using flow

cytometry," *American Journal of Respiratory Cell and Molecular Biology*, vol. 49, no. 2, pp. 180–189, 2013.

[27] P. Schnorrer, G. M. N. Behrens, N. S. Wilson et al., "The dominant role of CD8+ dendritic cells in cross-presentation is not dictated by antigen capture," *Proceedings of the National Academy of Sciences of the United States of America*, vol. 103, no. 28, pp. 10729–10734, 2006.

[28] I. Daurkin, E. Eruslanov, J. Vieweg, and S. Kusmartsev, "Generation of antigen-presenting cells from tumor-infiltrated CD11b myeloid cells with DNA demethylating agent 5-aza-2'-deoxycytidine," *Cancer Immunology, Immunotherapy*, vol. 59, no. 5, pp. 697–706, 2010.

[29] Y. Kitahata, T. Kanuma, M. Hayashi et al., "Circulating nanoparticulate TLR9 agonist scouts out tumor microenvironment to release immunogenic dead tumor cells," *Oncotarget*, vol. 7, no. 31, pp. 48860–48869, 2016.

[30] A. Viola, A. Sarukhan, V. Bronte, and B. Molon, "The pros and cons of chemokines in tumor immunology," *Trends in Immunology*, vol. 33, no. 10, pp. 496–504, 2012.

[31] M. T. Chow and A. D. Luster, "Chemokines in cancer," *Cancer Immunology Research*, vol. 2, no. 12, pp. 1125–1131, 2014.

[32] R. Tokunaga, W. Zhang, M. Naseem et al., "CXCL9, CXCL10, CXCL11/CXCR3 axis for immune activation—a target for novel cancer therapy," *Cancer Treatment Reviews*, vol. 63, pp. 40–47, 2018.

[33] R. A. Kroczek and V. Henn, "The role of XCR1 and its ligand XCL1 in antigen cross-presentation by murine and human dendritic cells," *Frontiers in Immunology*, vol. 3, p. 14, 2012.

[34] R. E. Anderson, G. B. Olson, J. R. Autry, J. L. Howarth, G. M. Troup, and P. H. Bartels, "Radiosensitivity of T and B lymphocytes. IV. Effect of whole body irradiation upon various lymphoid tissues and numbers of recirculating lymphocytes," *Journal of Immunology*, vol. 118, no. 4, pp. 1191–1200, 1977.

[35] C. Belka, H. Ottinger, E. Kreuzfelder et al., "Impact of localized radiotherapy on blood immune cells counts and function in humans," *Radiotherapy and Oncology*, vol. 50, no. 2, pp. 199–204, 1999.

[36] A. M. Florea and D. Busselberg, "Cisplatin as an anti-tumor drug: cellular mechanisms of activity, drug resistance and induced side effects," *Cancers*, vol. 3, no. 1, pp. 1351–1371, 2011.

[37] T. Walle, R. Martinez Monge, A. Cerwenka, D. Ajona, I. Melero, and F. Lecanda, "Radiation effects on antitumor immune responses: current perspectives and challenges," *Therapeutic Advances in Medical Oncology*, vol. 10, 2018.

[38] Z. S. Guo, Z. Liu, D. L. Bartlett, D. Tang, and M. T. Lotze, "Life after death: targeting high mobility group box 1 in emergent cancer therapies," *American Journal of Cancer Research*, vol. 3, no. 1, pp. 1–20, 2013.

[39] S. R. Woo, L. Corrales, and T. F. Gajewski, "The STING pathway and the T cell-inflamed tumor microenvironment," *Trends in Immunology*, vol. 36, no. 4, pp. 250–256, 2015.

[40] K. Li, S. Qu, X. Chen, Q. Wu, and M. Shi, "Promising targets for cancer immunotherapy: TLRs, RLRs, and STING-mediated innate immune pathways," *International Journal of Molecular Sciences*, vol. 18, no. 2, 2017.

[41] A. Izaguirre, B. J. Barnes, S. Amrute et al., "Comparative analysis of IRF and IFN-alpha expression in human plasmacytoid and monocyte-derived dendritic cells," *Journal of Leukocyte Biology*, vol. 74, no. 6, pp. 1125–1138, 2003.

[42] E. Tomasello, K. Naciri, R. Chelbi et al., "Molecular dissection of plasmacytoid dendritic cell activation *in vivo* during a viral infection," *The EMBO journal*, vol. 37, no. 19, article e98836, 2018.

[43] X. Huang and Y. Yang, "Targeting the TLR9-MyD88 pathway in the regulation of adaptive immune responses," *Expert Opinion on Therapeutic Targets*, vol. 14, no. 8, pp. 787–796, 2010.

[44] C. Bode, M. Fox, P. Tewary et al., "Human plasmacytoid dendritic cells elicit a type I interferon response by sensing DNA via the cGAS-STING signaling pathway," *European Journal of Immunology*, vol. 46, no. 7, pp. 1615–1621, 2016.

[45] S. Hervas-Stubbs, J. L. Perez-Gracia, A. Rouzaut, M. F. Sanmamed, A. Le Bon, and I. Melero, "Direct effects of type I interferons on cells of the immune system," *Clinical Cancer Research*, vol. 17, no. 9, pp. 2619–2627, 2011.

[46] R. M. Welsh, K. Bahl, H. D. Marshall, and S. L. Urban, "Type 1 interferons and antiviral CD8 T-cell responses," *PLoS Pathogens*, vol. 8, no. 1, article e1002352, 2012.

[47] R. F. V. Medrano, A. Hunger, S. A. Mendonca, J. A. M. Barbuto, and B. E. Strauss, "Immunomodulatory and antitumor effects of type I interferons and their application in cancer therapy," *Oncotarget*, vol. 8, no. 41, pp. 71249–71284, 2017.

[48] C. Havenar-Daughton, G. A. Kolumam, and K. Murali-Krishna, "Cutting edge: the direct action of type I IFN on CD4 T cells is critical for sustaining clonal expansion in response to a viral but not a bacterial infection," *Journal of Immunology*, vol. 176, no. 6, pp. 3315–3319, 2006.

[49] K. B. Nguyen, T. P. Salazar-Mather, M. Y. Dalod et al., "Coordinated and distinct roles for IFN-$\alpha\beta$, IL-12, and IL-15 regulation of NK cell responses to viral infection," *Journal of Immunology*, vol. 169, no. 8, pp. 4279–4287, 2002.

[50] J. B. Swann, Y. Hayakawa, N. Zerafa et al., "Type I IFN contributes to NK cell homeostasis, activation, and antitumor function," *Journal of Immunology*, vol. 178, no. 12, pp. 7540–7549, 2007.

[51] K. Kiefer, M. A. Oropallo, M. P. Cancro, and A. Marshak-Rothstein, "Role of type I interferons in the activation of autoreactive B cells," *Immunology and Cell Biology*, vol. 90, no. 5, pp. 498–504, 2012.

[52] L. Bracci, G. Schiavoni, A. Sistigu, and F. Belardelli, "Immune-based mechanisms of cytotoxic chemotherapy: implications for the design of novel and rationale-based combined treatments against cancer," *Cell Death and Differentiation*, vol. 21, no. 1, pp. 15–25, 2014.

[53] J. A. Wargo, A. Reuben, Z. A. Cooper, K. S. Oh, and R. J. Sullivan, "Immune effects of chemotherapy, radiation, and targeted therapy and opportunities for combination with immunotherapy," *Seminars in Oncology*, vol. 42, no. 4, pp. 601–616, 2015.

[54] H. Ma, S. Jin, W. Yang et al., "Interferon-alpha enhances the antitumour activity of EGFR-targeted therapies by upregulating RIG-I in head and neck squamous cell carcinoma," *British Journal of Cancer*, vol. 118, no. 4, pp. 509–521, 2018.

[55] F. Sabbatino, Y. Wang, G. Scognamiglio et al., "Antitumor activity of BRAF inhibitor and IFNα combination in BRAF-mutant melanoma," *Journal of the National Cancer Institute*, vol. 108, no. 7, article djv435, 2016.

[56] I. Rafique, J. M. Kirkwood, and A. A. Tarhini, "Immune checkpoint blockade and interferon-α in melanoma," *Seminars in Oncology*, vol. 42, no. 3, pp. 436–447, 2015.